

Research Article

Buffer Film Assisted Growth of Dense MWCNTs on Copper Foils for Flexible Electrochemical Applications

Udomdej Pakdee¹ and Boonchai Duangsawat²

¹*Division of Physics, Department of Science, Faculty of Science and Technology, Rajamangala University of Technology Krungthep, Bangkok 10120, Thailand*

²*Division of Chemistry, Department of Science, Faculty of Science and Technology, Rajamangala University of Technology Krungthep, Bangkok 10120, Thailand*

Correspondence should be addressed to Udomdej Pakdee; udomdej.p@gmail.com

Received 5 August 2017; Revised 20 October 2017; Accepted 25 October 2017; Published 21 November 2017

Academic Editor: Andrew R. Barron

Copyright © 2017 Udomdej Pakdee and Boonchai Duangsawat. This is an open access article distributed under the Creative Commons Attribution License, which permits unrestricted use, distribution, and reproduction in any medium, provided the original work is properly cited.

The novel Inconel buffer films were prepared on copper foils using unbalance direct current (DC) magnetron sputtering. These films were employed as buffer layers for supporting the dense growth of multiwalled carbon nanotubes (MWCNTs). Thermal chemical vapor deposition (CVD) with metal alloys such as stainless steel (SS) type 304 films was considered to synthesize MWCNTs. To understand the effectiveness of these buffer films, the MWCNTs grown on buffer-free layer were carried out as a comparison. The main problem such as the diffusion of catalysts into the oxide layer of metal substrate during the CVD process was solved together with a creation of good electrical contact between substrate and nanotubes. The morphologies, crystallinities, and electrochemical behaviors of MWCNTs grown on Inconel buffer films with 304 SS catalysts revealed the better results for applying in flexible electrochemical applications.

1. Introduction

Since the landmark paper of discoverable multiwalled carbon nanotubes (MWCNTs) was published in 1991 [1]. The MWCNTs have been extensively of interest for various researchers for several decades. Because of their excellent properties, they are considered as candidates in nanotechnological works such as sensors, composite materials, capacitors, and many others. The MWCNTs can be well grown on semiconducting and insulating substrates such as silicon or silicon oxide [2–5]. Thermal chemical vapor deposition (CVD) with the classical transition metal catalysts including nickel (Ni), iron (Fe) and cobalt (Co) was popularly operated to synthesize the MWCNTs [6]. There are many reports that metal alloy based on Fe such as stainless steel (SS) is one of the best catalysts for CNT growth [7–10]. For electrode works, the MWCNT were scraped off and mixed with a binder and a solvent. The resulting MWCNTs were then coated on a conductive substrate. And then, they were test for electrode performance. The problem with this technique is the high

value of total electrode resistance due to their various contact layers. Moreover, the use of binders has an effect on the overall surface morphology of MWCNTs. Therefore, the direct growth of MWCNTs on the metal substrate for creation a good electrical contact between substrate and MWCNTs is challenging. Typically, copper substrate has been suggested to be the great choice in electrode applications. Copper (Cu) is well known as the common conductive materials. It has been employed in various works due to its outstanding thermal and electrical conductivity properties. However, the MWCNTs grown directly on Cu substrates in a large scale production have demonstrated problems due to their low activity with Cu surface [11]. Therefore, the addition of catalysts including Ni, Fe, Co, and their alloys has been necessary [12, 13]. For the dense growth of MWCNTs on a metal substrate, the prevention of catalyst diffusion into the oxide layers of the substrate is required. The low reaction temperature (<700°C) was chosen to reduce the diffused effect [11]. But decreasing the reaction temperature also decreases the crystalline quality

TABLE 1: Sputtered conditions for deposition of Inconel and 304 SS films.

Parameters	Inconel buffer film	304 SS catalytic film
Base pressure (mbar)	5×10^{-5}	5×10^{-5}
Working pressure (mbar)	3×10^{-3}	3×10^{-3}
Substrate temperature ($^{\circ}\text{C}$)	R.T	R.T
Distance between the target and the substrate (cm)	10	10
Ar flow rates (sccm)	5	5
DC power (W)	217	280
Sputtering time (s)	60	30

of MWCNTs [14]. Metal, oxide, and nitride films such as Al, Ta, SiO_2 , TiO_2 , MgO, Al_2O_3 , and TiN have been used as a buffer layer due to their thermal barrier properties [15–25]. For Al_2O_3 buffer film, it has been applied as a classical buffer layer for supporting the aligned growth of MWCNTs [16, 17, 26]. This layer can be prepared using different techniques. Thermal oxidation technique has been widely employed to form an oxide layer on the top surface of Al film [26]. However, this is a major cause for the rough surface of substrates. As the initial surface of substrate is rough, the synthesized MWCNTs are nonalignment and high defect structures [26]. Therefore, this is a disadvantage for MWCNT applications in powerful effectiveness. Sputtering technique with reactive gas was reported as a good technique for preparation of smooth Al_2O_3 films. The sputtered Al_2O_3 films were considered to achieve a smooth initial buffer surface for more effective MWCNT growth [26]. However, the barrier layers may increase the electrical contact resistance between the copper substrates and the nanotubes. In the recent year, titanium nitride films have been conducted as the buffer layer with the low contact resistance in MWCNT growth [22]. Kim et al. investigated electrochemical behaviors of MWCNTs grown on Inconel coated Cu foils using the mixture of xylene and ferrocene [26]. They discussed the fact that the Fe nanoparticles from the ferrocene can be delivered during the CVD process for increasing the lifetime of catalyst action. This result has an effect on the growth of MWCNTs in vertical alignment. They also reported in other works that MWCNTs grown on Cu foil using only Ni catalyst without Inconel layer were poor [11]. Therefore, the power density and specific capacitance values of the double layer capacitors could be developed from the dense growth of MWCNTs on Cu substrates using Inconel layers.

In this work, the dense MWCNTs were synthesized on Cu foils using 304 SS films as catalysts. During the CVD process, thin Inconel® Alloy 600 sputtered films were considered as important buffer layers for preventing the diffusion of catalysts into the oxide layers of Cu substrate. These results were compared with the MWCNTs obtained from buffer-free layer. The experimental data show that the use of thin Inconel film could be a novel way to improve the quantity and quality of MWCNTs grown on metal substrates. The investigations of surface morphologies, crystallinities, and electrochemical behaviors of MWCNTs grown on Inconel buffer films with 304 SS catalysts would be represented.

2. Materials and Methods

2.1. Preparation of Buffer and Catalytic Films. A $1 \times 1 \text{ cm}^2$ copper foil (Brastech Company) with a thickness of $50 \mu\text{m}$ was used as a substrate. The foil was ultrasonically cleaned in acetone first followed by methanol for 15 min and dried with nitrogen before loading into the chamber of a DC magnetron sputtering. To obtain a smooth buffer layer, active Inconel buffer film was first sputtered onto the copper foil at room temperature (R.T). Pure Ar (99.99%) was employed as the sputtered gas with flow rates of 5.0 sccm. Before the deposition, the target was sputter-cleaned in Ar plasma for 5 min to remove the oxides and impurities on the top surface of target. An Ar flow rate during the sputtered cleaning was set at 5 sccm under a total pressure of 3×10^{-3} mbar, while electrical power on the targets was kept at 0.4 A and ~ 540 V. During deposition, the Inconel target was supplied by DC power supply for 60 s to achieve 45 ± 3 nm thick Inconel buffer film. And then, these films were ultrasonically cleaned in acetone and methanol again before coating with 10 nm thick 304 SS film as catalysts. The details of all deposited conditions kept in this study are shown in Table 1.

2.2. Growth of MWCNTs. The catalytic substrate was ultrasonically cleaned and dried with nitrogen before loading into a horizontal stainless steel chamber of a home-built thermal CVD system. This home-built system was reported in the previous work of authors [27]. The chamber was evacuated with a rotary pump until the base pressure inside the chamber was less than 10^{-2} mbar. Then, argon was fed into the chamber with a flow rate of 200 sccm. Meanwhile, the controlled valve of a rotary pump was closed until the pressure in the chamber was higher than atmospheric pressure indicating, by a dial vacuum gauge, that the drain valve was opened for gas exit. And then, the chamber was heated up to 770°C . The exhausted gas was cooled down by the water before it was drained out. Hydrogen (H_2) as reductive gas was injected into the chamber with a flow rate of 100 sccm for 30 min to etch the oxide on the substrate surface. The gas can promote the active sites on the top surface of substrate. After that, the acetylene (C_2H_2) was fed into the chamber with a flow rate of 60 sccm for 5 min. Finally, the MWCNTs were formed and they were cooled down using Ar with a flow rate of 100 sccm until it obtained the room temperature.

2.3. Characterization. Scanning electron microscopy (SEM) was used for the characterization of the surface morphology

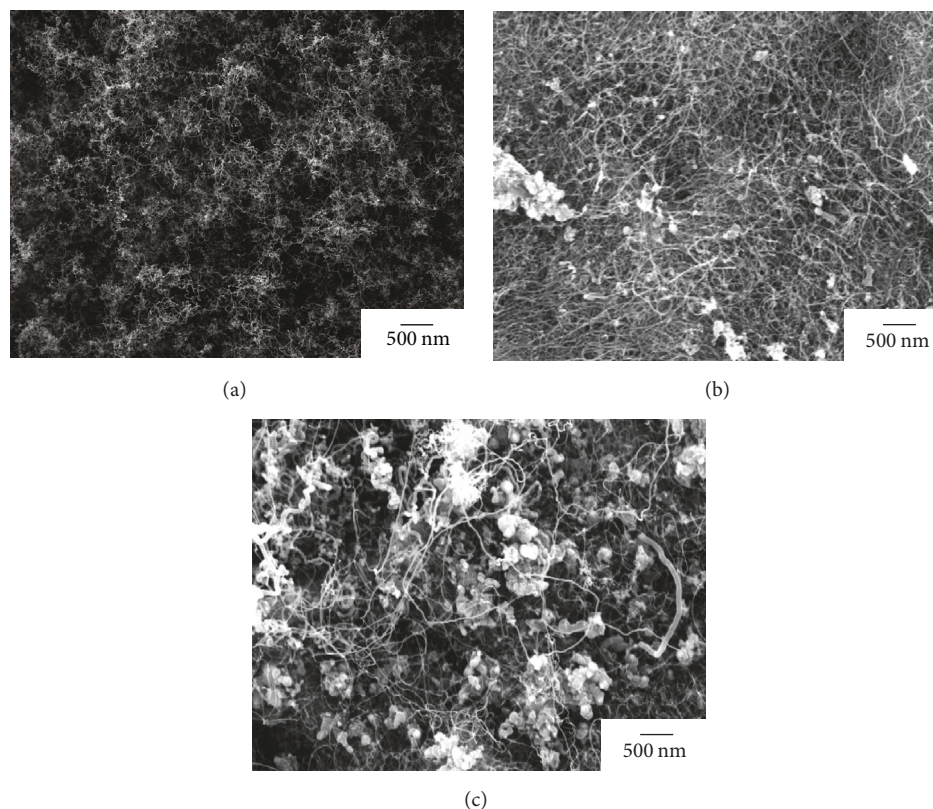


FIGURE 1: SEM images of the MWCNTs grown on different Inconel layer thicknesses with 304 SS catalysts for temperature at 770°C : (a) 10 ± 5 nm, (b) 45 ± 3 nm, and (c) 75 ± 5 nm.

of MWCNTs and catalytic substrates using a Quanta 450 FEI SEM working at 30 kV. X-ray diffraction (XRD) was employed to reveal the main elemental existence of buffer films. Transmission electron microscopy was conducted to indicate the inner and outer diameters of MWCNTs using a Hitachi HT 7700 TEM operating at accelerating voltages of 120 kV and 200 kV. X-ray photoelectron spectroscopy (XPS) was used for characterization of the chemical composition using a ULVAC-PHI XPS calibrated by using the C1s peak (284.6 eV) as a reference. Raman spectroscopy on the measurements of MWCNTs was done using a Perkin Elmer Spectrum GX FT-Raman to study the quality of MWCNTs presented by I_D/I_G ratios. The electrochemical behaviors were examined using an Autolab PGSTAT 30 potentiostat. The measurements were performed in the three electrodes within 1 M LiCl solution (Gammaco Company) as the electrolyte. The synthesized MWCNTs on buffer layers were used as the working electrode operated with a platinum foil as the counter electrode and standard silver/silver chloride (Ag/AgCl) as the reference electrode. Before the measurement, the back side of all electrodes was coated with insulating epoxy for preventing the charge build up effect.

3. Results and Discussion

Figure 1 shows the SEM images of MWCNTs grown on Cu foil substrates with 10 nm thick 304 SS catalysts using different

Inconel buffer layer thicknesses of 10 ± 5 nm, 45 ± 3 nm, and 75 ± 5 nm. It can be observed that the thicknesses of Inconel buffer layer in the range of 10 ± 5 nm and 75 ± 5 nm represent the poor growth of MWCNTs. Additionally, as the buffer layer thickness increases, the density of MWCNTs tends to vary. For the case of 75 ± 5 nm Inconel layer, many amorphous carbon structures can be observed. The optimum buffer layer thickness for the highest density of MWCNTs was observed for the case of the 45 ± 3 nm Inconel layer. Although some amorphous big particles also can be observed, it is mostly dense growth of MWCNTs. From the literature [28], the Inconel film thickness in the range of 10–12 nm was represented in the best alignment and density of CNT forests. In that case, the iron catalyst was supplied by mixing ferrocene with the xylene. Therefore, the catalysts were always added during the CVD process. For our work, the catalyst was coated and placed prior to the CVD process and no catalyst was added during the CVD process. This may be the reason why the best possible results are different. The best result that there was high density of MWCNTs on the substrate warranted a more thorough investigation. The Inconel film with a thickness of 45 ± 3 nm was chosen to understand what truly happened to the 304 SS catalyst film during the MWCNT growth.

Before the CVD process, the buffer film was first deposited on a Cu foil substrate. It can be seen in Figure 2(a) that the thickness of an Inconel buffer film in cross-sectional

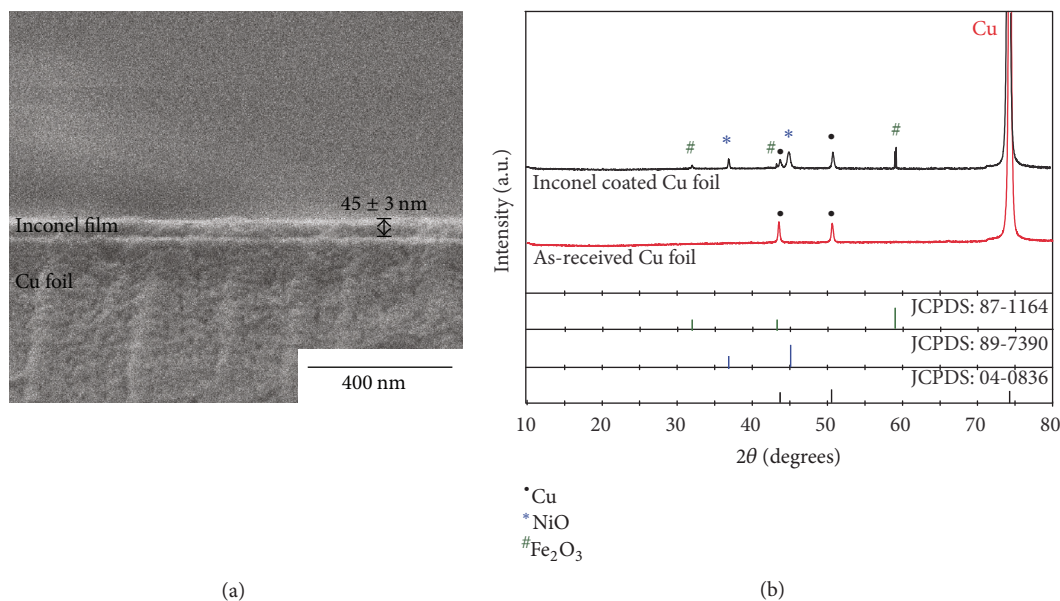


FIGURE 2: Representative images of (a) cross-sectional SEM and (b) XRD patterns for Inconel buffer film deposited on Cu foil.

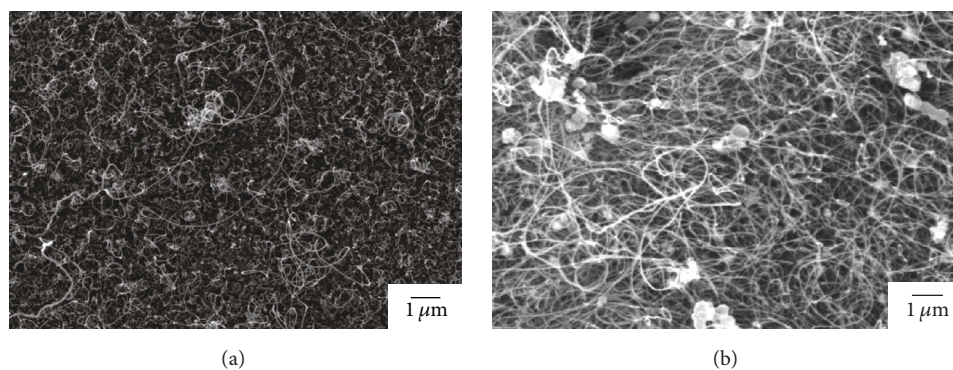


FIGURE 3: SEM images of MWCNTs grown on Cu foils with 304 SS catalysts for temperature at 770°C using (a) buffer-free layer and (b) Inconel buffer layer.

SEM images is in the range of 45 ± 3 nm analyzing with the ImageJ public software program. Figure 2(b) shows the XRD patterns of the as-received Cu foil substrate and Inconel buffer film deposited on the Cu foil. The XRD pattern of the as-received Cu foil surface only illustrates the existence of Cu element according to JCPDS file number 04-0836. For Inconel buffer film, the XRD pattern illustrates the presence of nickel-oxide (NiO) and iron-oxide (Fe_2O_3) according to JCPDS file numbers 89-7390 and 87-1164, respectively.

Figure 3 shows the SEM images of MWCNTs grown on Cu foil substrates with 10 nm thick 304 SS catalysts using buffer-free layer (Figure 3(a)) and Inconel buffer layer (Figure 3(b)). This allows us to more easily observe that the MWCNTs grown on the Inconel buffer film tend to grow in a more dense growth, while those grown on the free-buffer layer tend to be less in terms of growth density.

Figure 4 shows the distributions in diameter of MWCNTs with buffer-free layer and Inconel buffer layer conditions. The diameter of MWCNTs was analyzed by SEM images with

the ImageJ public software program. For both conditions, the diameter of MWCNTs was found to be in the range of 10–60 nm. The average diameters of MWCNTs grown on Cu foils with buffer-free layer and Inconel buffer layer conditions are 33 and 36 nm, respectively. However, the good alignment of MWCNTs was grown on Cu foils with Inconel buffer layer. This result indicated that the introduction of an Inconel buffer layer to the growth condition increased alignment levels in the atomic carbon structure.

The poor growth of MWCNTs grown on Cu foil surface for the buffer-free condition was investigated more thoroughly. A 10 nm 304 SS film was chosen to study what correctly occurred to the as-received catalytic film during the CVD process. The 304 SS film on the Cu substrate was heated in the CVD chamber to duplicate all conditions without the carbon source. It is observed from the SEM images in Figure 5(a) that the substrate surface was lacking the catalytic nanoparticles. The disappearance of catalytic nanoparticles could be discussed by the fact that the catalysts may diffuse

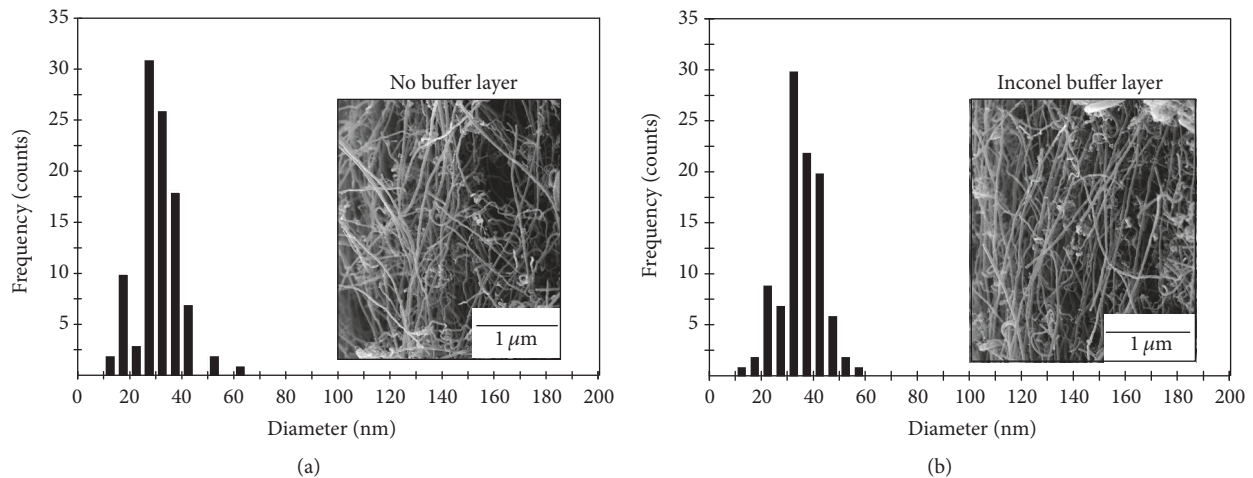


FIGURE 4: SEM images and distributions in diameter of MWCNTs grown on Cu foils with 304 SS catalysts for temperature at 770°C using (a) buffer-free layer and (b) Inconel buffer layer.

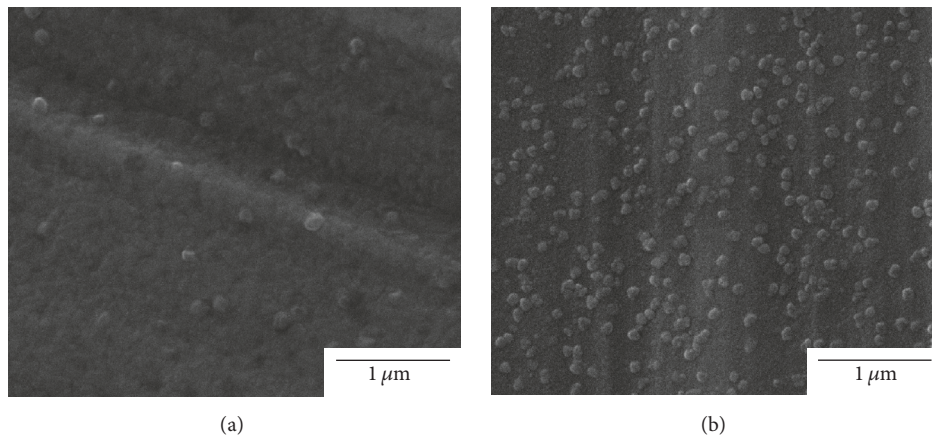


FIGURE 5: SEM images of the 304 SS catalyst distribution on Cu foils after annealing for temperature at 770°C using (a) buffer-free layer and (b) Inconel buffer layer.

into the oxide layer on the surface of Cu substrate during the CVD process [11, 23]. In contrast, the higher density of catalytic nanoparticles can be observed in Figure 5(b). These particles acted as catalysts for the dense growth of MWCNTs.

There have been many papers reporting that Inconel film and Inconel substrate can be used as catalysts for the MWCNT growth [28, 29]. To understand the effect of Inconel film as buffer layer on the growth of MWCNTs, a bare surface (Inconel film layer deposited on Cu foil) was further investigated. Although the film thickness of Inconel is up to 45 ± 3 nm, the experimental results are similar to the case of 10 nm thick stainless steel as catalysts with buffer-free layer. The disappearance of catalytic nanoparticles and the poor growth of MWCNTs are represented as shown in Figure 6. The diffusion of the catalysts into the oxide layer of Cu is also discussed in this case. Therefore, the growth of MWCNTs on Cu foil at 770°C using metal alloy catalysts (SS or Inconel) with buffer-free layer is poor.

Based on the SEM images of Figures 3(b) and 4(b), there are some amorphous big particles beside the MWCNTs. To study the formation of some amorphous big particles, the remaining substrate surface for the rest of Figure 5(b) is shown in Figure 7. In this figure, the distribution of 304 SS catalysts can be observed in full space. However, some big particles were distributed beside the nanoparticles. It was discussed that the nearby SS nanoparticles could be merged and formed into a single larger particle at high temperature [30]. For the nanoparticles, they cause the formation of MWCNTs with better coverage in contrast to the big particles where big amorphous carbon growth was observed. The formation of amorphous carbon structures on the big catalyst was identified where the catalyst island size is larger than the diffusion length of carbon atoms [11]. Therefore, the catalytic particles must be small enough to allow for the growth of the MWCNTs.

As a result, it has been discussed using the Ostwald ripening rate. The Ostwald ripening is a phenomenon in

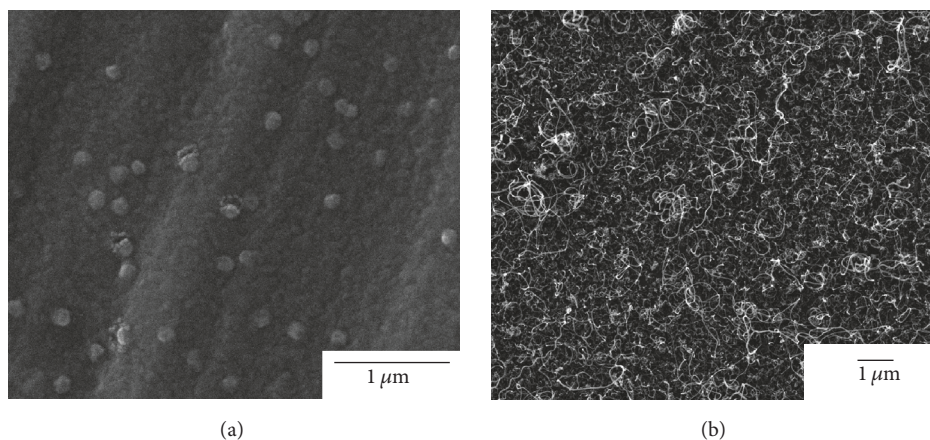


FIGURE 6: SEM images of (a) the 45 nm Inconel layer post 770°C anneal region showing catalytic nanoparticles and (b) the MWCNTs grown on a bare surface (Inconel deposited on Cu foil).

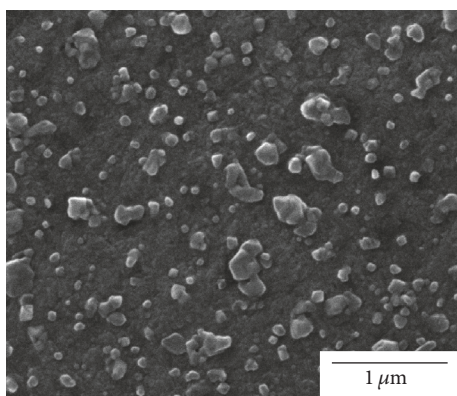


FIGURE 7: SEM image representative of the remainder surface for the 304 SS catalyst distribution on Cu foils after annealing for temperature at 770°C using Inconel buffer layer.

solid or liquid solutions of inhomogeneous small particles on the larger particle surface. The lower Ostwald ripening rates derived from the higher surface energies of catalysts deposited on the lower surface energies of substrates. These lower rates may lead to a good catalyst distribution [29–31]. Therefore, Inconel (metal alloy based on Ni) has lower surface energy (1.7 J/m^2) [29] relative to the Cu surface (1.9 J/m^2) [29]. Essentially, the 304 SS metal alloy based on iron with the high surface energy of 3.5 J/m^2 [29] should be used as the effective catalysts on an Inconel layer for the lower Ostwald ripening rates. This cause may likely induce the dense growth of MWCNTs on Inconel buffer layer.

Some of MWCNTs were ultrasonically removed from the substrate with ethanol. It was examined using TEM and XPS. The TEM images in low and high resolutions represent the MWCNTs in all growth conditions as shown in Figures 8(a) and 8(b). It can be confirmed that the products are multiwalled carbon nanotubes with the inner diameter and outer diameter of $12 \pm 5 \text{ nm}$ and $35 \pm 5 \text{ nm}$, respectively. These statistical measurements are calculated from ImageJ program

software in five different areas from each of the three samples at low resolution of TEM.

The content of carbon was investigated using XPS spectra as shown in Figure 9. The atomic concentrations of Cls and OIs were calculated using CasaXPS software. The calculated values were slightly different in the event of buffer layer and buffer-free layer cases. The atomic concentration of Cls increased from 98.3 at.% to 98.4 at.% when the substrate was applied with the Inconel layer, whereas the concentration of OIs decreased from 1.7 at.% to 1.6 at.%. However, these high values of carbon contents do not indicate that all structures are perfect MWCNTs. A more investigation was warranted using an XPS deconvolution process. The Cls peak was deconvoluted using the Gaussian-Lorentzian fitting curve. The binding energies of 284.3 eV [32], 285.3 eV [32], 286.2 eV [32, 33], and 287.5 eV [32, 33] correspond to the bonds of $\text{sp}^2 \text{ C=C}$, $\text{sp}^3 \text{ C-C}$, C-O, and O-C=O which were also observed. The sp^3 and sp^2 atomic concentration values were also calculated from the CasaXPS software. For the buffer-free layer case, the calculated values of sp^3 and sp^2 are 14.1 and 71.6 at.%, respectively. In contrast, the sp^3 and sp^2 values for the applied Inconel layer case are 11.2 and 78.1 at.%, respectively. These results can clearly show that the majority of the deposition is sp^2 hybridized carbon. However, the further examination suggests that the difference in the applied Inconel layer can change in sp^3/sp^2 ratio. As the Inconel buffer layer is applied, the sp^3/sp^2 ratio decreases from 0.19 to 0.14.

Figure 10 shows the Raman spectra from 500 to 3000 cm^{-1} of MWCNTs grown on buffer-free layer and Inconel buffer layer using 304 SS catalysts. The three manners of D, G, and G' peaks were observed at about 1344, 1582, and 2545 cm^{-1} , respectively. The D peak ($\sim 1350 \text{ cm}^{-1}$) is indicative amorphous carbonaceous impurities with sp^3 carbon bonds and broken sp^2 carbon bonds in the nanotube sidewalls [26]. The G peak ($\sim 1580 \text{ cm}^{-1}$) is relative to the graphitic nature of carbon [26]. The intensity ratio of I_D/I_G can be widely used to claim the degree of crystallinity or purity of the MWCNTs grown on substrates. The G' peak

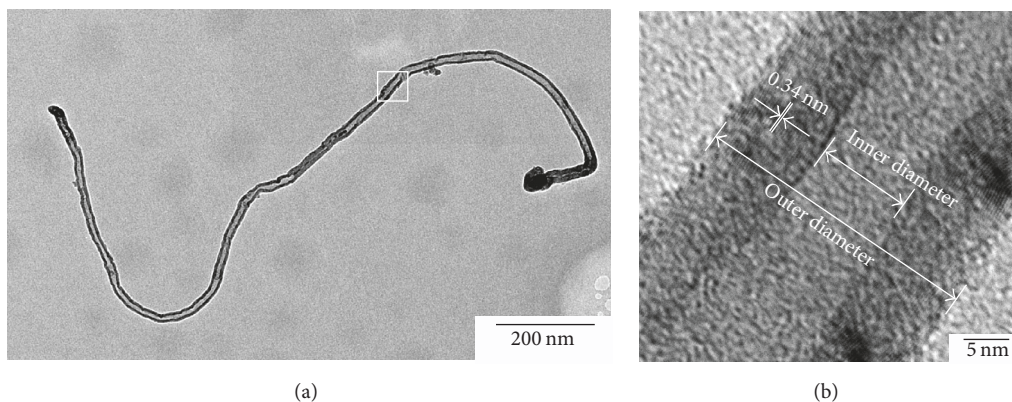


FIGURE 8: Representative images of (a) low resolution TEM and (b) high resolution TEM.

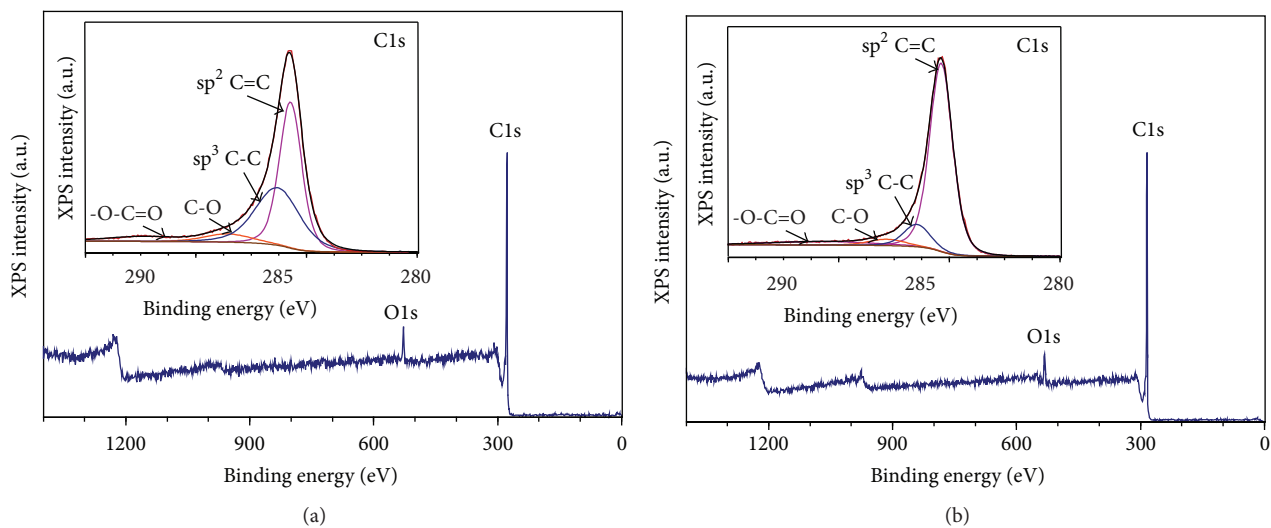


FIGURE 9: XPS spectra of MWCNTs grown on Cu foils with 304 SS catalysts for temperature at 770°C using (a) buffer-free layer and (b) Inconel buffer layer.

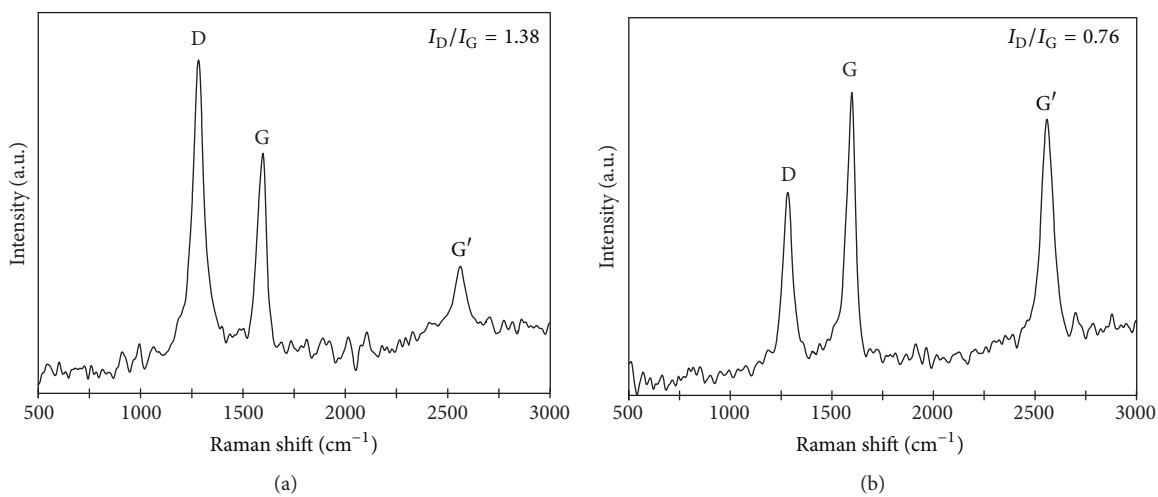


FIGURE 10: Raman spectra of MWCNTs grown on (a) buffer-free layer and (b) Inconel buffer layer.

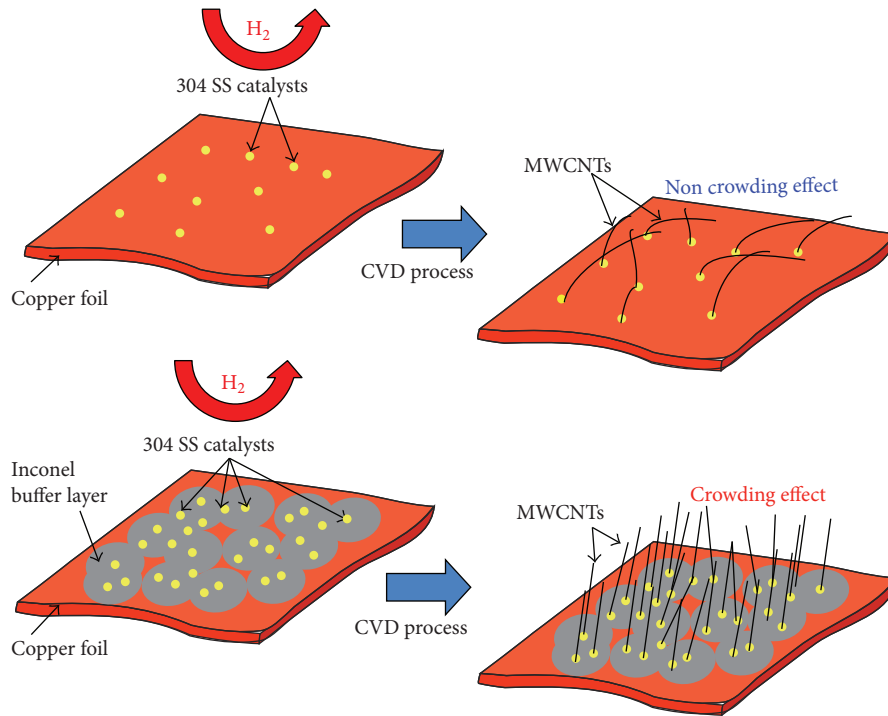


FIGURE 11: Schematic images of the differences in growth mechanism of MWCNTs grown on free-buffer layer and Inconel buffer layer conditions.

(2500–2900 cm^{-1}) can be used to reveal the second order of two-phonon scattering process in the creation of an inelastic phonon [5]. The peak has extensively indicated the long range order of perfection or purity in graphitic bonds [12, 13, 34, 35]. The I_D/I_G ratios of 1.38 and 0.76 were observed for MWCNTs grown on buffer-free Cu foil and Inconel coated Cu foil as shown in Figures 10(a) and 10(b), respectively. The I_D/I_G ratios are indicative of the existence of some defects and amorphous carbons. It is clearly seen that a buffer layer of Inconel can promote the better quality of MWCNTs. This is strongly consistent with the sp^3/sp^2 ratio obtained from XPS. Furthermore, the appearance of a strong long range ordered G' peak is significant for reference in a MWCNT charge storage performance [34]. A sharp G' peak was observed in Figure 10(b) indicating that the MWCNTs grown on Inconel coated Cu foil are important for a good action in the charge storage capability.

Figure 11 shows schematic illustrations of the different mechanisms of MWCNTs grown on buffer-free layer and Inconel buffer layer conditions. The high density of catalytic nanoparticles obtained from Inconel buffer condition is an important factor for supporting the dense growth of MWCNTs. This growth tends to grow with a higher degree of alignment due to the crowding effect [12]. This effect is generally known where van der Waals forces among close-by CNT neighbors cause them to all grow vertically to the substrate. Therefore, the high growth yield is also important in CNT alignment.

Electrochemical measurements were conducted to prove that the MWCNTs grown on Inconel buffer layer using 304

SS as catalysts present a good electrical conductivity for electrochemical electrode applications. Figure 12(a) shows the cyclic voltammograms (CV) at four different scan rates of 5, 10, 50, and 100 mV s^{-1} . The almost rectangular-like shape of all CV curves was observed. The rectangular shape of CV is well known where it is base of capacitor behavior. Moreover, it was also observed in Figure 12(b) that the MWCNTs grown on Inconel buffer layer do not greatly fall down even after 100 and 500 cycles. Thus, it is ideally taken for a steady electrode in charge and discharge works. Figure 12(c) shows the charge-discharge curves to demonstrate the properties of MWCNTs grown on Inconel buffer layer. This electrode was operated at a constant current of 1 mA. The curves reveal the mirror-like images and slight a drop of uppermost signals. Therefore, the conductivity and the stability of this electrode are good. Specific capacitance for the electrode was calculated according to the following formula (1):

$$C_{\text{sp}} = \frac{I}{m (dv/dt)}, \quad (1)$$

where I represents the discharge current in A, m refers to the mass of electrode in g, and dv/dt is the discharge slope obtained from Figure 12(c). The calculation of C_{sp} for MWCNTs grown on Inconel buffer layer is 1.54 F g^{-1} . This calculated value may not be the highest achieved nowadays [36–38]. However, the authors try to present the fact that thin Inconel film may be the good candidate in combination with other carbon-based electrodes for the powerful capacitor performances.

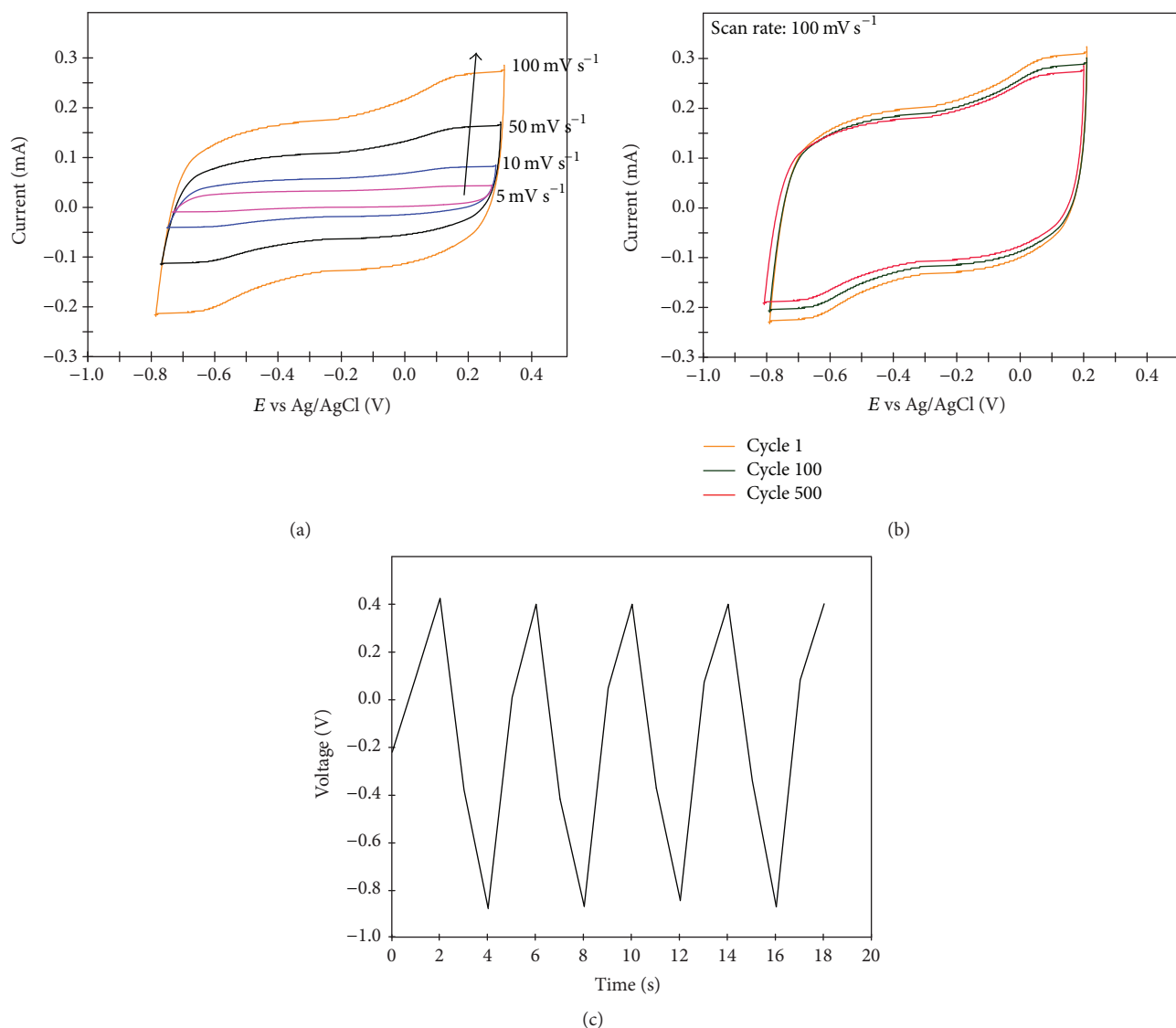


FIGURE 12: (a) Cyclic voltammograms of MWCNTs grown on Inconel buffer layer at four scan rates of 5, 10, 50 and 100 mV s⁻¹, (b) cycle 1, cycle 100 and cycle 500 of CV measurements at a scan rate of 100 mV s⁻¹ and (c) charge-discharge curves of MWCNTs grown on Inconel buffer layer obtained at a constant current of 1 mA.

4. Conclusions

This work presents the binder-free growth of MWCNTs on Cu foils using 304 SS catalysts by simple thermal CVD. The Inconel films were represented as important buffer layers for preventing the diffusion of catalysts into the oxide layer of metal substrates. The yield of MWCNTs grown on Inconel buffer layers is higher than that grown on buffer-free layer. Furthermore, Inconel is the best choice for the good alignment and good quality of MWCNTs grown on Cu foils. The CV results show the high stability and good conductivity of MWCNTs grown on Inconel coated Cu foils. The calculated value of specific capacitance for MWCNT-based electrode using 1 M LiCl as electrolyte is 1.54 F g⁻¹. Finally, this finding may lead to new alternative for the selection of buffer materials in the dense growth of MWCNTs used for flexible electrochemical electrodes and other flexible applications.

Conflicts of Interest

The authors declare that there are no conflicts of interest regarding the publication of this paper.

Acknowledgments

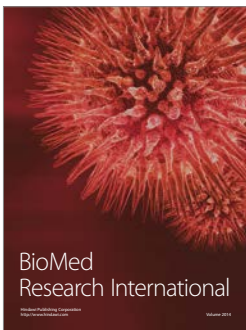
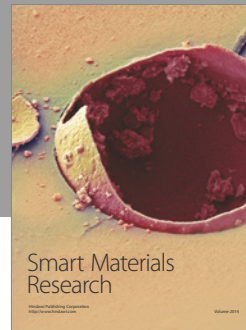
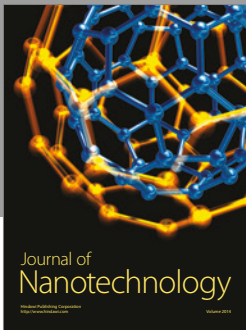
This work was supported by Research and Development Institute, Rajamangala University of Technology Krungthep, Thailand.

References

- [1] S. Iijima, "Helical microtubules of graphitic carbon," *Nature*, vol. 354, no. 6348, pp. 56–58, 1991.
- [2] M. Pérez-Cabero, A. Monzón, I. Rodríguez-Ramos, and A. Guerrero-Ruiz, "Syntheses of CNTs over several iron-supported

- catalysts: influence of the metallic precursors,” *Catalysis Today*, vol. 93–95, pp. 681–687, 2004.
- [3] J. Jiang, T. Feng, X. Cheng et al., “Synthesis and growth mechanism of Fe-catalyzed carbon nanotubes by plasma-enhanced chemical vapor deposition,” *Nuclear Instruments and Methods in Physics Research Section B: Beam Interactions with Materials and Atoms*, vol. 244, no. 2, pp. 327–332, 2006.
 - [4] M. Wienecke, M.-C. Bunescu, K. Deistung, P. Fedtke, and E. Borchartd, “MWCNT coatings obtained by thermal CVD using ethanol decomposition,” *Carbon*, vol. 44, no. 4, pp. 718–723, 2006.
 - [5] S. S. Madani, K. Zare, M. Ghoranneviss, and A. S. Elahi, “Synthesis of carbon nanotubes using the cobalt nanocatalyst by thermal chemical vapor deposition technique,” *Journal of Alloys and Compounds*, vol. 648, pp. 1104–1108, 2015.
 - [6] C. J. Lee, J. Park, and J. A. Yu, “Catalyst effect on carbon nanotubes synthesized by thermal chemical vapor deposition,” *Chemical Physics Letters*, vol. 360, no. 3–4, pp. 250–255, 2002.
 - [7] W. Z. Li, D. Z. Wang, S. X. Yang, J. G. Wen, and Z. F. Ren, “Controlled growth of carbon nanotubes on graphite foil by chemical vapor deposition,” *Chemical Physics Letters*, vol. 335, no. 3–4, pp. 141–149, 2001.
 - [8] V. Martínez-Hansen, N. Latorre, C. Royo, E. Romeo, E. García-Bordejé, and A. Monzón, “Development of aligned carbon nanotubes layers over stainless steel mesh monoliths,” *Catalysis Today*, vol. 147, pp. S71–S75, 2009.
 - [9] C. Zhuo, X. Wang, W. Nowak, and Y. A. Levendis, “Oxidative heat treatment of 316L stainless steel for effective catalytic growth of carbon nanotubes,” *Applied Surface Science*, vol. 313, pp. 227–236, 2014.
 - [10] B. Kim, H. Chung, K. S. Chu, H. G. Yoon, C. J. Lee, and W. Kim, “Synthesis of vertically-aligned carbon nanotubes on stainless steel by water-assisted chemical vapor deposition and characterization of their electrochemical properties,” *Synthetic Metals*, vol. 160, no. 7–8, pp. 584–587, 2010.
 - [11] G. Atthipalli, R. Epur, P. N. Kumta et al., “The effect of temperature on the growth of carbon nanotubes on copper foil using a nickel thin film as catalyst,” *Thin Solid Films*, vol. 519, no. 16, pp. 5371–5375, 2011.
 - [12] G. Atthipalli, H. Wang, and J. L. Gray, “Catalyst-assisted vertical growth of carbon nanotubes on Inconel coated commercial copper foil substrates versus sputtered copper films,” *Applied Surface Science*, vol. 273, pp. 515–519, 2013.
 - [13] G. Atthipalli, R. Epur, P. N. Kumta, M. Yang, J.-K. Lee, and J. L. Gray, “Nickel catalyst-assisted vertical growth of dense carbon nanotube forests on bulk copper,” *The Journal of Physical Chemistry C*, vol. 115, no. 9, pp. 3534–3538, 2011.
 - [14] C. J. Lee, J. Park, Y. Huh, and J. Yong Lee, “Temperature effect on the growth of carbon nanotubes using thermal chemical vapor deposition,” *Chemical Physics Letters*, vol. 343, no. 1–2, pp. 33–38, 2001.
 - [15] A. Cao, P. M. Ajayan, G. Ramanath, R. Baskaran, and K. Turner, “Silicon oxide thickness-dependent growth of carbon nanotubes,” *Applied Physics Letters*, vol. 84, no. 1, pp. 109–111, 2004.
 - [16] T. De Los Arcos, M. G. Garnier, J. W. Seo, P. Oelhafen, V. Thommen, and D. Mathys, “The influence of catalyst chemical state and morphology on carbon nanotube growth,” *The Journal of Physical Chemistry B*, vol. 108, no. 23, pp. 7728–7734, 2004.
 - [17] T. De los Arcos, M. G. Garnier, P. Oelhafen et al., “Strong influence of buffer layer type on carbon nanotube characteristics,” *Carbon*, vol. 42, no. 1, pp. 187–190, 2004.
 - [18] G.-Y. Xiong, D. Z. Wang, and Z. F. Ren, “Aligned millimeter-long carbon nanotube arrays grown on single crystal magnesia,” *Carbon*, vol. 44, no. 5, pp. 969–973, 2006.
 - [19] H. C. Lee, P. S. Alegaonkar, D. Y. Kim et al., “Multi-barrier layer-mediated growth of carbon nanotubes,” *Thin Solid Films*, vol. 516, no. 11, pp. 3646–3650, 2008.
 - [20] T. Ohashi, R. Kato, T. Tokune, and H. Kawarada, “Understanding the stability of a sputtered Al buffer layer for single-walled carbon nanotube forest synthesis,” *Carbon*, vol. 57, pp. 401–409, 2013.
 - [21] W.-Y. Wu, F.-Y. Teng, and J.-M. Ting, “The effect of an Al underlayer on Fe-Si thin film catalysts for the improved growth of carbon nanotubes,” *Carbon*, vol. 49, no. 13, pp. 4589–4594, 2011.
 - [22] C. Jin, M. Delmas, P. Aubert et al., “Nanostructured tantalum nitride films as buffer-layer for carbon nanotube growth,” *Thin Solid Films*, vol. 519, no. 12, pp. 4097–4100, 2011.
 - [23] J. García-Céspedes, S. Thomasson, K. B. K. Teo et al., “Efficient diffusion barrier layers for the catalytic growth of carbon nanotubes on copper substrates,” *Carbon*, vol. 47, no. 3, pp. 613–621, 2009.
 - [24] T.-C. Wu and S.-H. Chang, “Temperature enhanced growth of ultralong multi-walled carbon nanotubes forest,” *Current Applied Physics*, vol. 9, no. 5, pp. 1117–1121, 2009.
 - [25] S. Shukrullah, N. M. Mohamed, and M. S. Shaharun, “Optimum temperature on structural growth of multiwalled carbon nanotubes with low activation energy,” *Diamond and Related Materials*, vol. 58, article no. 6428, pp. 129–138, 2015.
 - [26] J. S. Kim, Y.-W. Jang, and I.-T. Im, “Growth of vertical carbon nanotubes according to the Al₂O₃ buffer layer preparation,” *Journal of Industrial and Engineering Chemistry*, vol. 19, no. 5, pp. 1501–1506, 2013.
 - [27] U. Pakdee, S. Chiangga, S. Suwannatus, and P. Limsuwan, “Growth of MWCNTs on flexible stainless steels without additional catalysts,” *Journal of Nanomaterials*, vol. 2017, Article ID 5672728, 11 pages, 2017.
 - [28] G. Atthipalli, R. Epur, P. N. Kumta, and J. L. Gray, “Ferrocene and Inconel assisted growth of dense carbon nanotube forests on copper foils,” *Journal of Vacuum Science & Technology B*, vol. 29, no. 4, article 04D102, 2011.
 - [29] R. M. Silva, A. C. Bastos, F. J. Oliveira et al., “Catalyst-free growth of carbon nanotube arrays directly on Inconel® substrates for electrochemical carbon-based electrodes,” *Journal of Materials Chemistry A*, vol. 3, no. 34, pp. 17804–17810, 2015.
 - [30] R. L. Vander Wal and L. J. Hall, “Carbon nanotube synthesis upon stainless steel meshes,” *Carbon*, vol. 41, no. 4, pp. 659–672, 2003.
 - [31] W. Cho, M. Schulz, and V. Shanov, “Growth and characterization of vertically aligned centimeter long CNT arrays,” *Carbon*, vol. 72, pp. 264–273, 2014.
 - [32] T. I. T. Okpalugo, P. Papakonstantinou, H. Murphy, J. McLaughlin, and N. M. D. Brown, “High resolution XPS characterization of chemical functionalised MWCNTs and SWCNTs,” *Carbon*, vol. 43, no. 1, pp. 153–161, 2005.
 - [33] V. Datsyuk, M. Kalyva, K. Papagelis et al., “Chemical oxidation of multiwalled carbon nanotubes,” *Carbon*, vol. 46, no. 6, pp. 833–840, 2008.
 - [34] G. Atthipalli, Y. Tang, A. Star, and J. L. Gray, “Electrochemical characterization of carbon nanotube forests grown on copper foil using transition metal catalysts,” *Thin Solid Films*, vol. 520, no. 5, pp. 1651–1655, 2011.

- [35] R. A. DiLeo, B. J. Landi, and R. P. Raffaele, "Purity assessment of multiwalled carbon nanotubes by Raman spectroscopy," *Journal of Applied Physics*, vol. 101, no. 6, article 064307, 2007.
- [36] S. Dörfler, I. Felhösi, T. Marek et al., "High power supercap electrodes based on vertical aligned carbon nanotubes on aluminum," *Journal of Power Sources*, vol. 227, pp. 218–228, 2013.
- [37] R. Reit, J. Nguyen, and W. J. Ready, "Growth time performance dependence of vertically aligned carbon nanotube supercapacitors grown on aluminum substrates," *Electrochimica Acta*, vol. 91, pp. 96–100, 2013.
- [38] M. Noked, S. Okashy, T. Zimrin, and D. Aurbach, "Thick vertically aligned carbon nanotube/carbon composite electrodes for electrical double-layer capacitors," *Carbon*, vol. 58, pp. 134–138, 2013.



Hindawi

Submit your manuscripts at
<https://www.hindawi.com>

